THE PUBLISHING HOUSE
OF THE ROMANIAN ACADEMY

GEONOMY
Research article

ALLANITE-(Ce) AND ITS ASSOCIATIONS, FROM THE DITRAU ALKALINE INTRUSIVE MASSIF, EAST CARPATHIANS, ROMANIA

Paulina HIRTOPANU[1*], Jens C. ANDERSEN[2], Robert J. FAIRHURST[2] and Gyula JAKAB[3]

[1] Dept.Mineralogy, University of Bucharest, Romania
[2] University of Exeter, Camborne School of Mine, UK
[3] IG Mineral Gheorgheni, Romania
*paulinahirtopanu@hotmail.com

Received March 27, 2013

The Ditrau alkaline intrusive complex (DAIC) is situated within the crystalline rocks of the inner part of the East Carpathians. It has a distinct ring structure and a succession of magmatic events from gabbroic and dioritic magma to syenitic and various postmagmatic events as well, developed between a Triassic extensional stage and a Jurassic rifting stage. The DAIC has a high petrographic complexity and a great diversity of mineral occurrences. More than 200 new minerals were recently identified, many of them being first occurrences in Romania. The rare element minerals which were determined in DAIC belong to the following classes, in the predominant order: I.LREE(Y)-carbonates; II. Nb, Ta, REE(Y),Ti, Zr, Th, U-oxides III.REE(Y)-Phosphates; IV. REE-(Y), Th, Zr, Pb-Silicates. Among silicates, the following minerals occur in DAIC, specially in Jolotca area: allanite-(Ce), thorite, thorogummite, cerite-(Ce), chevkinite-(Ce), törnebohmite-(Ce), stillwellite-(Ce), tritomite-(Ce), britholite-(Ce) and Th-zircon. Allanite-(Ce) occurs as a constituent mineral in mineralizing Jolotca area and as an accessory one in the rest of the massif. The chemical composition of allanite-(Ce) has high Fe_2O_3 content, showing oxidizing conditions for its genesis. The effect of changing redox conditions could be one possible cause of the neoformation of allanite-(Ce) on the other REE-silicates. The allanite-(Ce) is quite commonly attacked by fluids and transformed into REE-fluorcarbonates minerals, most often into bastnasite-(Ce). The opposite allanitisation process of REE-carbonates is widely spread in DAIC and it is illustrated in many pictures. Also, the allanite-(Ce) can form on monazite-(Ce) and this transformation process is reversible. It presents many generations, having specific the continuous decreasing of REE contents from the old to the new members, shown by their microprobe analyses. Oscillatory zoning of allanite-(Ce) seen only in backscattered electron images, would result from changes in temperature, pressure and REE-concentrations in fluid, during its crystallization. The textural relations of the REE-silicates, mineralogical and chemical evidence demonstrate that hydrothermal processes were responsible for the REE mineralization at DAIC.

Key words: allanite-(Ce), monazite-(Ce), chevkinite-(Ce), törnebohmite-(Ce), cerite-(Ce), stillwellite-(Ce), tritomite-(Ce), hydrothermal activity.

LOCATION, GEOLOGICAL SETTING AND PETROGRAPHY

The Ditrau alcaline intrusive complex (DAIC) is situated in the central crystalline rock series on the inner part of the East Carpathians, Romania (46°48' N, 25°30E). It is a massif of intermediate size and displays an elliptical form (19/14Km), localized in a G8 crustal fracture zone, that is the border line between the crystalline Mesozoic belt to the East and the Neogene volcanic belt to the West. The metamorphic rocks around the border zone of the massif belong mostly to Cambrian metamorphic Tulghes Group. A thermal contact aureole (hornfels with andalusite, cordierite, biotite, grossularite, wollastonite, corindon, spinel, etc.) has developed in the country rocks.

The massif presents a distinct ring structure (Streckeisen, 1960). The outer ring is formed by alkali-granites, alkali-syenites and nepheline-syenites, essexites, generally red in color, with gradual transitions between these rocks.The intermediate ring-dyke consists of foliated, sometimes schistose essexites which are banded by alkali-syenites being cut by nepheline-syenite veins by which they have been hybridised and metasomatically transformed. The large body of Ditrau essexites (nepheline gabbros) of both rings contain small lenses of ultrabasites at several places and show a gradual transitions to the alkali-syenites. The central stock (6 km in diameter) is formed by white, coarse grained nepheline syenites with abundant cancrinite and primary calcite. Abundant sodalite is found in veinlets or penetrating the rock and replacing the nepheline. Smaller masses of white nepheline-syenite with cancrinite and sodalite occurr at several places in the intermediate and outer ring-dykes up to the contact and even in the immediate contact aureole. The lamprophyres (camptonites and spessartites) dykes cut sharply the rocks of the outer and intermediate rings, but are lacking in the central stock. Aplitic and pegmatitic rocks are frequent especially in the white nepheline syenites to which they show gradual transitions. At several places, sodalite and cancrinite-sodalite-nepheline syenite pegmatites can be found; such rocks were termed “ditroites” by Streckeisen (1960). Also, the tinguaites (alkali feldspars, nepheline and alkali pyroxenes and amphiboles) rich in cancrinite are specially frequent in the central stock. Small veins of diverse carbonates are found in various rocks described above.

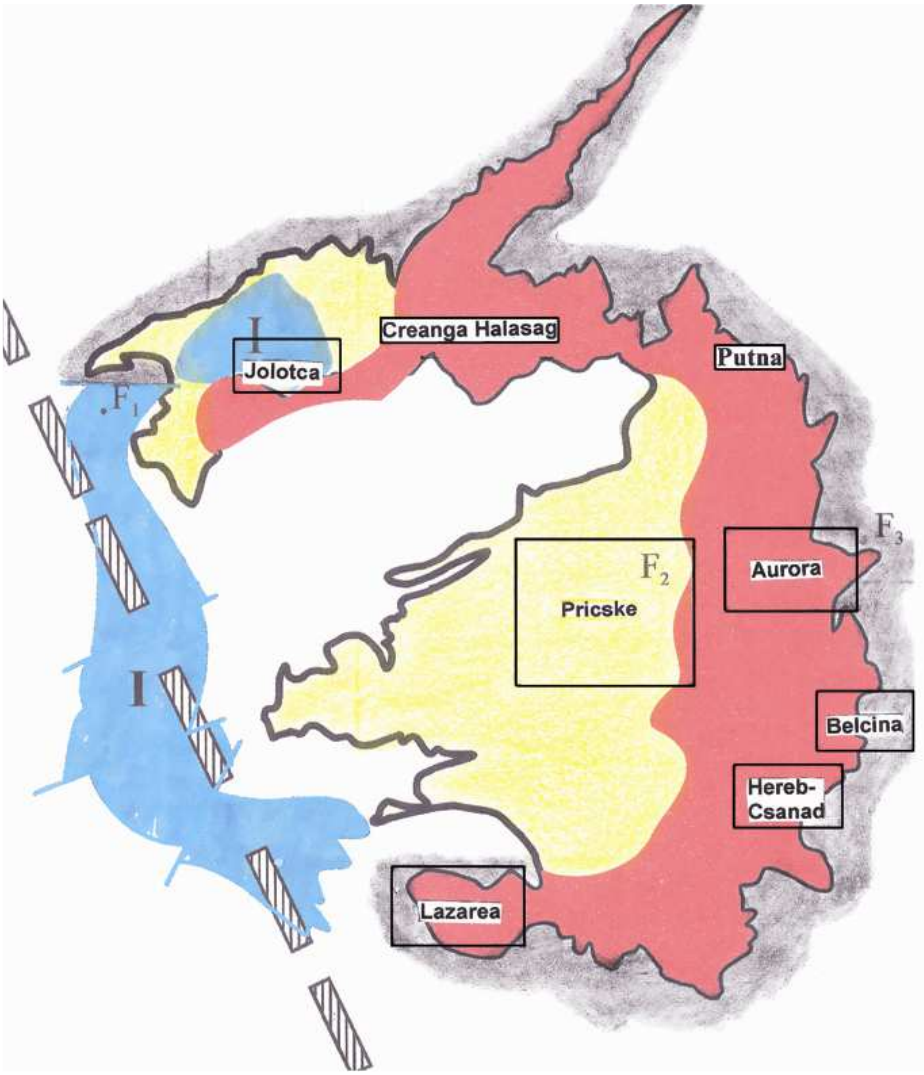

Fig 1. The schematic geological map of Ditrau alkaline massif with **mineralization areas**: hornblendite-diorite complex (blue), red syenite (red), white nepheline syenite (yellow), Tulghes Group (grey), **F** = fault, **G8**=crustal fracture (hachure interrupted line) (acc. to Jakab, G.).

The succession of the magmatic events was as follows: gabbroic and dioritic magma intrusion, followed by intrusion of syenitic magmas and the granitic rocks on the margins of the massif. The most important event was the rise of nepheline-bearing magmatic melts, fluid and hydrothermal solutions, which produced widespread hybridization and metasomatic changes that occurred in the massif in the later stages of its formation. A gas phase composed mainly of CO_2 was evolved, producing cancrinite and primary calcite and later of Cl, producing sodalite. The final stage of the intrusion are later rare nepheline aplite and pegmatite, and lamprophyres (mainly camptonites). The sodic character of alkaline magmatism maintained to the last fractionations of initial magma as albitisation, natrolitisation, analcimisation processes. The high Na comes probable from carbonatite bearing alkaline magmas which initially was made by Na carbonates. Also, alkali pyroxenes with many generations aegirine I, earlier than nepheline (in which it forms inclusions) to late aegirine and/or acmite and amfiboles (arfvedsonite-riebeckite) rich in Na are present as a late forming mineral phases in fenite rocks.

The structure of the massif is complicated by the succession of magmatic events from gabbroic and dioritic magma to syenitic and various postmagmatic events as well. According to Krautner & Bindea (1996) the emplacement history of DAIC is the folowing: (1) a mantle derived gabbroic magma (230 Ma) emplaced under extensional regime, carrying ultramafic mantle xenoliths, forming an outer ring; (2) intrusion of a crustal syentic magma (196 Ma), producing foliated rocks as well as hybridisation with gabbroic rocks; (3) a nepheline syenite intrusion (160 Ma), forming a central stock but pervasively penetrating the older rocks in the marginal parts as well. It has a multistages evolution developed mainly between a Triassic extensional stage and a Jurassic rifting stage. We complete this succession of magmatic events in DAIC, with carbonatite intrusion that followed after alkaline intrusion and has been used the same pathways of the preceding alkaline silicate melt. The carbonatites, originated from mantle, are exclusively linked with extension structures, as is DAIC. It affiliation to anorogene alkaline magmas explains their general feature Nb>>Ta. It is known that the association of carbonatites and alkalic rocks is by far the most important primary source of Nb and REE(Y). The DAIC represent the end of long lasting fractionation processes in the crust and deep upper mantle, respectively. This explains the modest dimensions of Ditrau intrusion and its enrichment with incompatible elements. However, the presence of carbontites allows us to name this complex as Ditrau carbonatite alkaline intrusive complex.

MINERALOGY

The high petrographic complexity of Ditrau massif is doubled by a great diversity of mineral occurrences. In addition of the 85 mineral species previously mentioned (Constantinescu & Anastasiu, 1977; Jakab, 1998; Constantinescu, 1999) the occurrence has been proved to contain a lot more minerals (over 200), some of them REE and Y minerals as well as Th, U, Nb, Ta, Zr, Ti minerals (Hirtopanu & Bermanec, 2000; Hirtopanu *et al.*, 2003; Hirtopanu & Udubasa, 2003; Hirtopanu, 2006a 2006b; Hirtopanu *et al.*, 2010a; 2010b). The rare elements minerals presented belong to the following 4 classes, in the predominant order: **REE(Y)–Carbonates**; Nb, Ta, REE(Y), **Ti, Zr, Th, U–Oxides**; **REE(Y)–Phosphates**; **REE(Y), Th, Zr, Pb –Silicates** (Hirtopanu et al., 2010b). They occur in some small mineralization areas (Lazarea, Hereb-Cianod, Ditrau Valley/Pricske, Aurora, Putna, Creanga Halasag) and in two big vein mineralization areas, Jolotca and Belcina (Fig 1). The biggest Jolotca occurrence from the NV of the massif is of vein type and comprises a complex sulphides mineralization. The rare elements mineralizations followed after sulphides, almost all the rare element minerals being developed as veins in sulphides, as a late hydrothermal phases.

The Jolotca rare elements mineralization has a gangue of ferrodolomite, ankerite, siderite and calcite. The other occurrence of vein type is the Belcina, less bigger than Jolotca, situated outside of the Ditrau massif at SE, in the surrounding metamorphic rocks of the Tulghes Group, at 2.5 km distance from the intrusive massif (Jakab, 1998) (Fig. 1). The Belcina occurrence comprises a complex mineralization, different from that reported in Jolotca. It is mostly constituted of Th silicates and Y-phosphates, less zircon, niobian rutile, ferrocolumbite, Y-fluorite, less sulphides. The most common important minerals in DAIC are microcline, albite, oligoclase, Fe and Ti-biotite, phlogopite, muscovite, kaersutite, pargasite, hastingsite, riebeckite-arfvedsonite, augite, aegirine-augite, titanaugite, titanite, nepheline, cancrinite, sodalite, apatite, scapolite, pectolite, analcime, natrolite, wairackite, calcite, dolomite, ankerite. Generally, the rocks show enrichment in Ca, Na, Fe, Ti, P, Zr, CO_2, Cl and F indicating that these rocks represent a transition from alkaline to peralkaline character (or from miaskitic to agpaitic).

The allanite-(Ce) belong to silicates class together with dollaseite-(Ce) (?), thorite, thorogummite, chevkinite-(Ce), törnebohmite-(Ce), cerite-(Ce), stillwellite-(Ce), tritomite-(Ce), britholite-(Ce) and zircon.

PHYSICAL DESCRIPTION, MINERAL ASSOCIATIONS AND CHEMICAL COMPOSITION OF ALLANITE-(Ce)

Allanite-(Ce), $Ca(Ce,La)Al_2Fe(SiO_4)(Si_2O_7)O(OH)$, monoclinic; may be metamict. It forms coarse brown to black good crystals of few cm, being grown tabular, prismatic to acicular (Figs. 2–6); also may be granular, massive. It presents polysynthetic twinning, common on (100) (Fig. 7). In thin section it has a brown or green colour with strong pleochroism: pale olive-green, reddish brown (*X*); dark brown, brownish yellow (*Y*); dark reddish brown, greenish brown (*Z*) (Fig. 6). It has an imperfect cleavage on (001) and poor on (100) and (110). Biaxial (+) or (-) with a small 2V around 40^0. Known as an accessory mineral, the allanite-(Ce) occurs in Ditrău occurrences as a constituent one, especially in the Jolotca area (Figs. 2, 3, 5).

The rare earth minerals can be classified into the six classes based on the types of anionic groups in their structure (Miyawaki and Nakai, 1993). Allanite-(Ce), as an aluminosilicate, belongs to the four groups with other REE aluminosilicate minerals with crystal structure containing anionic groups of tetrahedral and octahedral ions. Also, to this group belong some titanosilicates, *e.g.* mosandrite.

In the Figure 5 is presented an image of the Dt18 scanned polished thin section with allanite-(Ce) occurring as vein in pyrite. In transmitted light this allanite-(Ce) has strong pleochroism such it can see in Figure 6, from yellow, green, pink, to red, brown, black colors.

Alteration or transformation of REE minerals has been observed in many hydrothermal systems. This is to be expected because fluids of variable composition and temperature may pass through the same system at various stages of its geological history (Giere, 1984). Therefore, should be studied both primary and secondary REE minerals to establish the evolution of each particular hydrothermal system. The Ditrau allanite-(Ce) is quite commonly attacked by fluids and transformed into REE-fluocarbonates minerals, most often into bastnäsite-(Ce). The bastnäsitisation of allanite can be described schematically, as follows: allanite+fluid↔bastnäsite+clay mineral± fluorite±magnetite± thorite, where the clay mineral is represented by kaolinite. The formation of thorite as a reaction product is due to the elevated Th contents commonly observed in allanite (Giere, 1996). In DAIC the most frequently is the reverse processes, the transformation of bastnäsite-(Ce)/synchysite-(Ce) in allanite-(Ce) (Figs. 8, 9). In Figure 8 (left) allanite-(Ce) replaces a big grain of synchysite-(Ce), the last one remains as relics in it. In Figure 8 (right) allanite-(Ce) grows marginally and on the cracks of the bastnäsite-(Ce) big crystal.

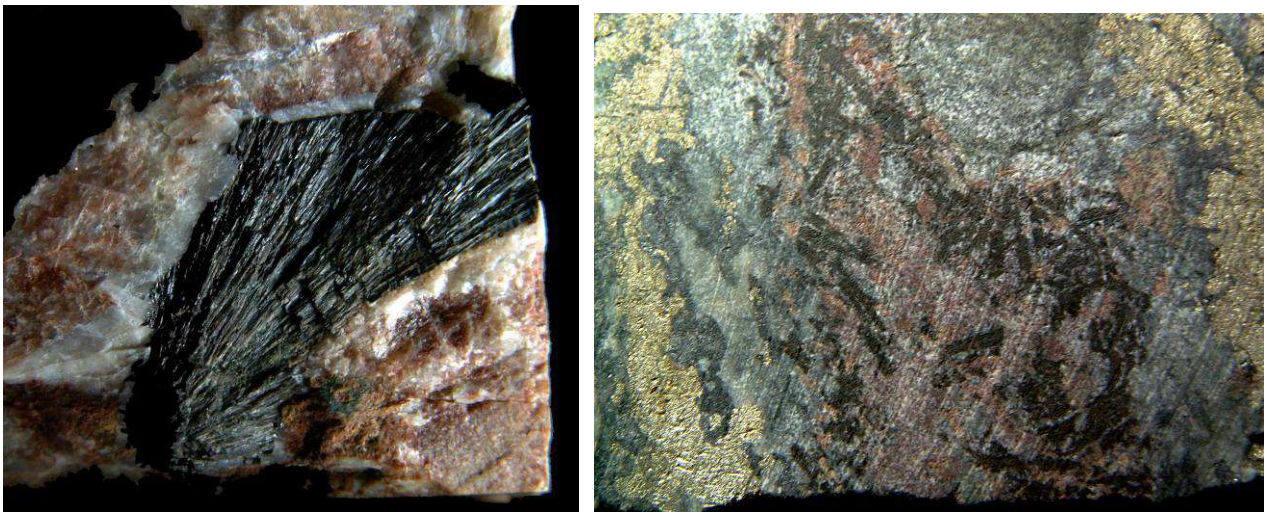

Fig. 2. Allanite-(Ce) vein in monazite-(Ce) (brick red) calcite (white), sample DT214 (left); allanite-(Ce) (black prisms), monazite-(Ce) (brick red), pyrite (yellow), chlorite (grey), calcite (light grey), sample DT55.

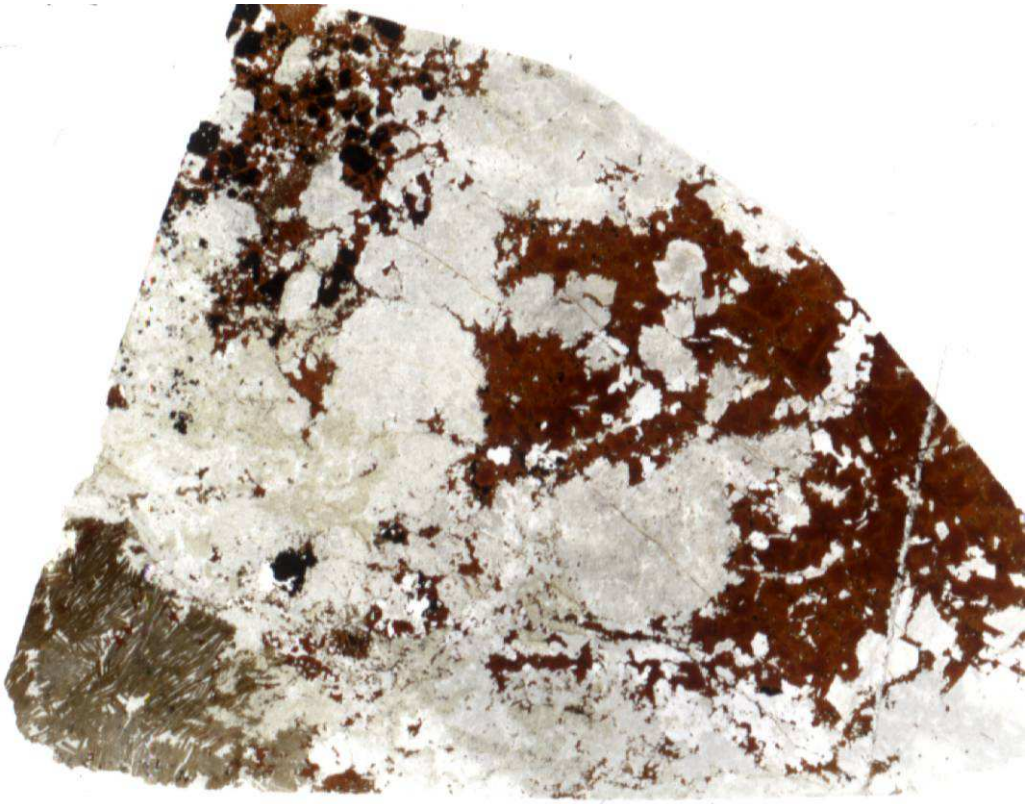

Fig. 3. Scanned polished thin section: acicular allanite-(Ce) (dark grey, left corner bottom), monazite-(Ce) (red), synchysite-(Ce) (light grey), calcite (white), pyrite (black), sample Dt6. See below the optical images of allanite-(Ce).

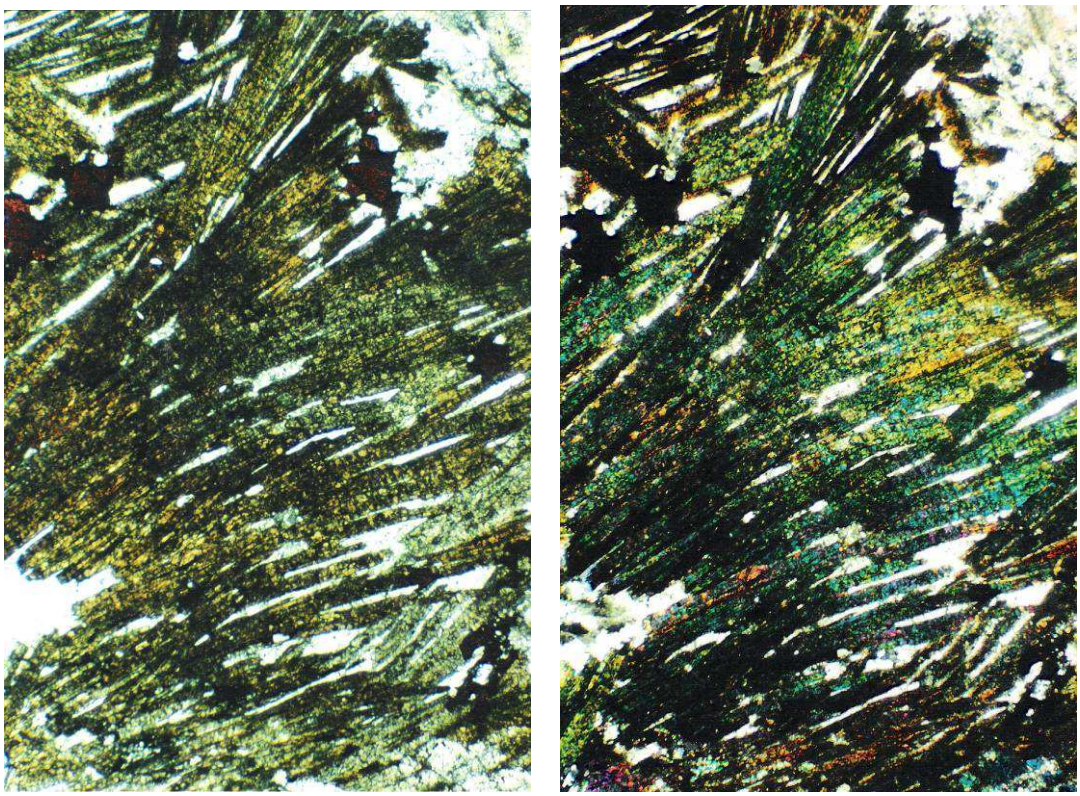

Fig. 4. Optical image of acicular allanite-(Ce) from Figure 3, red sphalerite (small, isotropic), thorite (red, small, anisotropic), NII (left) and N+ (right); see their microprobe analyses in Table 2.

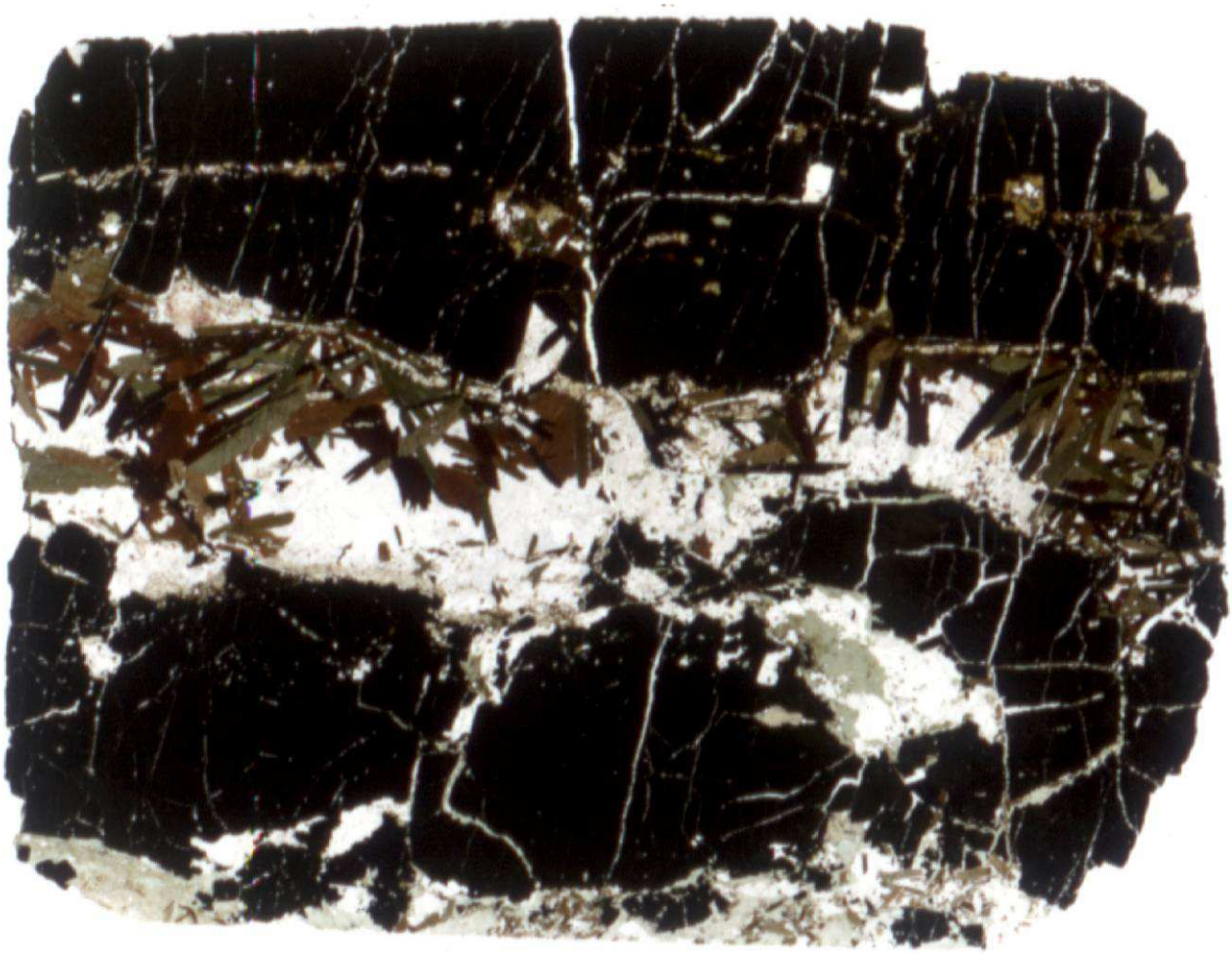

Fig. 5. Allanite-(Ce), brown, green, black prisms, vein in pyrite (black), calcite (white); scanned polished thin section Dt18; see below its optical images.

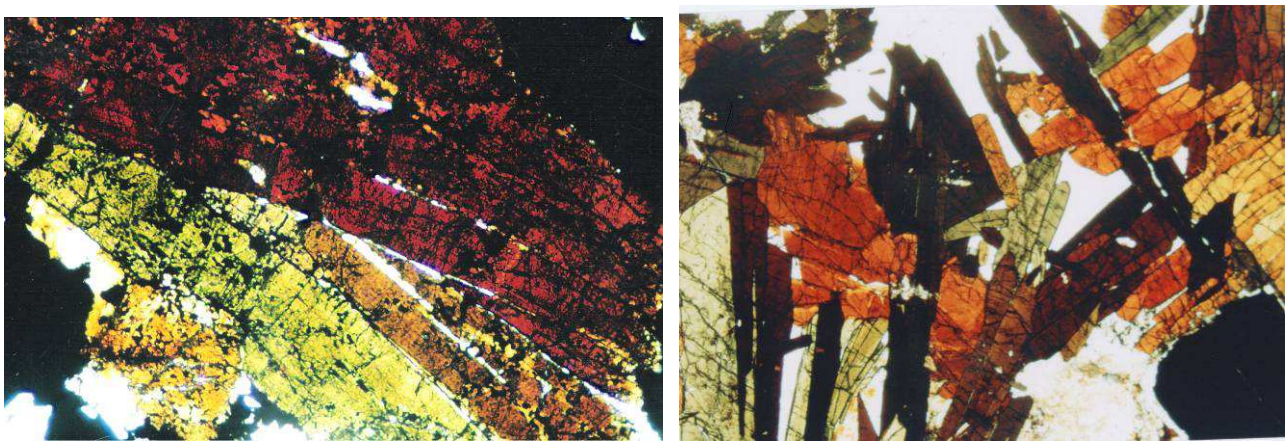

Fig. 6. Allanite-(Ce) prisms with high pleochroism, sample pyrite (black, isometric), NII, Dt18; See their composition in Table 2.

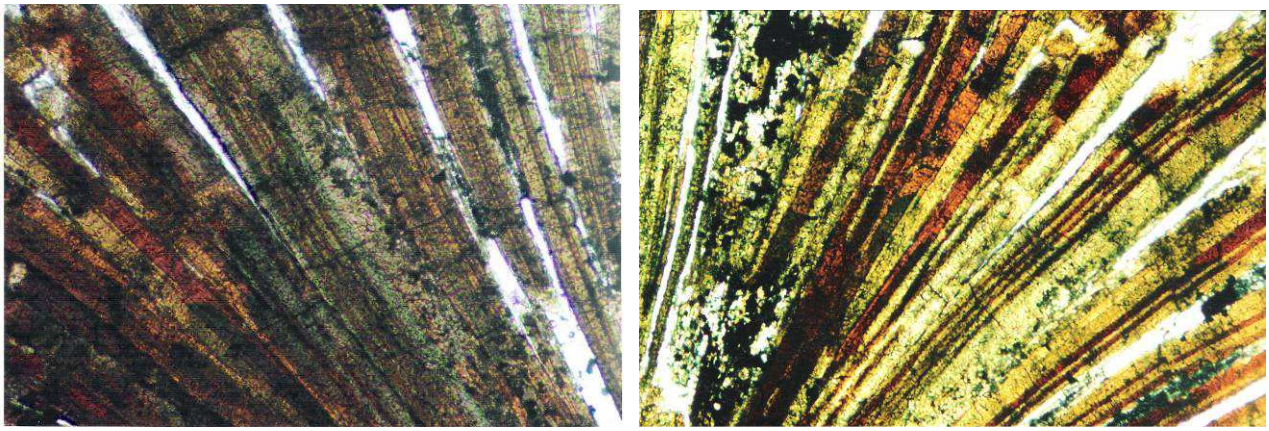

Fig. 7. Allanite-(Ce) with polysinthetic twinning, sample Dt19A (left) and Dt19 (right), N+.

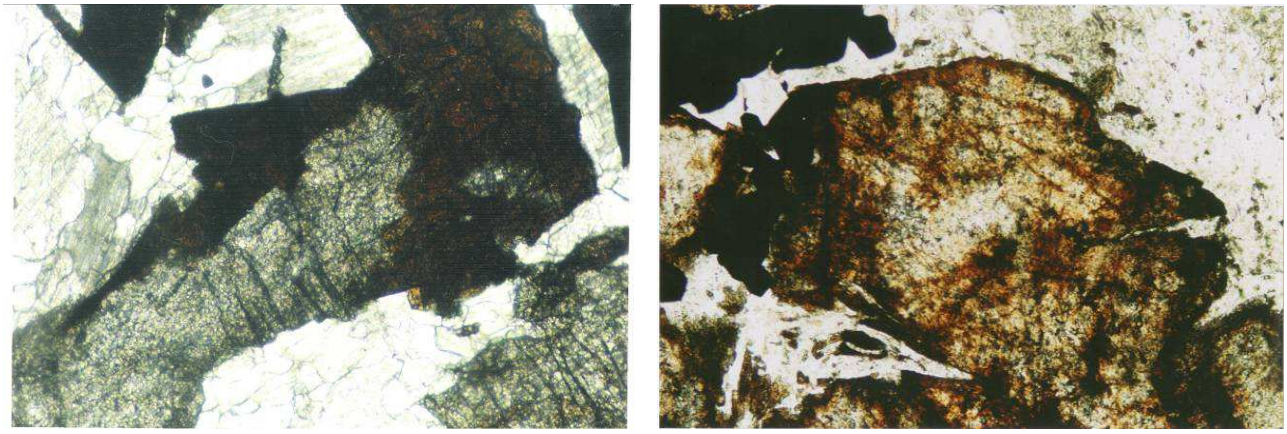

Fig. 8. Synchysite-(Ce) (grey prisms) altered in allanite-(Ce) (dark red), calcite (white), Dt212 (left); bastnasite-(Ce) (big crystal, rose) allanitized marginal and on the cracks (red), ferrocolumbite (small black grains), Dt8 (right), NII.

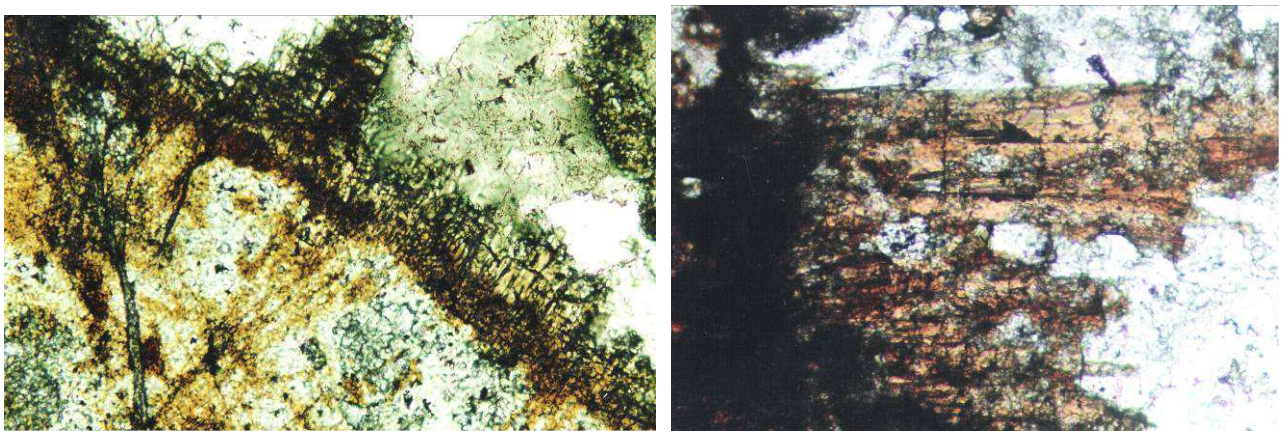

Fig. 9. Allanite-(Ce), small prisms grown perpendicular on big bastnäsite-(Ce) prism (yellow grey), Dt19/2 (left); allanite-(Ce) (pink prisms) grown perpendicular on chevkinite-(Ce) (black) and with bastnäsite-(La) inclusions (grey), sample Dt53/1. See their chemical composition in Table 1.

In the Figure 9 (left), the very narrow strip of allanite-(Ce) microgranular brown area, near bastnäsite-(Ce), has a high REE content, than that of the marginal with small yellow prisms. Here occur two allanite-(Ce) generation, with evident diminution of REE content. The pink big prisms allanite-(Ce) from Figure 9 (right), grown perpendicular on chevkinite-(Ce), in sample Dt53/1, have bastnäsite-(La) inclusions/veins, with La_2O_3 more than Ce_2O_3. The new formed bastnäsite-(La), occurring in the new formed allanite-(Ce) has the following chemical

composition: La_2O_3=51.254, Ce_2O_3=41.152, Nd_2O_3= 7.595 (%wt). This bastnäsite-(La) is formed on/with allanite-(Ce), which in its turn was formed on chevkinite-(Ce) and it appears as the last REE-carbonate generation. Also, inside of the newly formed allanite-(Ce) or in bastnäsite-(La) there occur small grains of red thorite, as a new product resulting by transformation of chevkinite-(Ce) with some Th content. These thorite inclusions have the following representative microprobe composition: SiO_2 = 17.010, ThO_2 = 82.990 (%wt). Also, the thorite could result and as a reaction product of the transformation of allanite-(Ce) with elevated Th contents, commonly observed in this mineral.

The allanite-(Ce) are associated with monazite-(Ce) (Figs. 2 ,3, 11, 12), bastnäsite-(Ce), törnebohmite-(Ce) (Fig. 14), chevkinite-(Ce) (Fig. 9), pyrochlore, niobian rutile, sphalerite, pyrite, galena. The association of allanite-(Ce) or other RE minerals, with sulphides, like sphalerite pyrite, galena, was explained by many researchers. In the H_2S-rich hydrothermal fluids, the formation of REE minerals may additionally be influenced by the crystallization of sulphides minerals; in several geological environments the REE appear to have been trapped at the site of sulphides precipitation (Gieré, 1996). However, at these sites the REE are not incorporated into sulphide minerals, but rather into accessory RE minerals or minerals with a high affinity for REE (Gieré, 1996). These minerals are texturally closely associated with sulphides, indicating that the deposition of REE from the hydrothermal fluids, could be genetically related to the crystallization of base metal sulphides. Barnes (1979) considered a chloride rich hydrothermal fluids in which ore forming elements such as Fe, Cu, Zn, Pb are carried as chlorides complexes. The conversion of metal chloride solution to sulphides minerals by reaction with H_2S, liberates H^+, which increases the acidity of hydrothermal fluid. The author considers that the deposition of the dissolved REE might then occurs in response to such a change in pH, induced by crystallization of the sulphides minerals.

The first microprobe Ditrau allanite-(Ce) analyses was made by Prof. Bermanec at Zagreb University laboratories (in Hirtopanu *et al.*, 2000). The results are shown in Table 2. The rest of all allanite-(Ce) analyses were made at CSM, Exeter University, UK (Table 3).

The allanite-(Ce) has in its formula the (OH) group which can reach until 2% wt and because it was not determined, which could explain the low totals of microprobe allanite-(Ce) analyses in Table 2. Also, the F, TiO_2, Y_2O_3 UO_2 contents were not determined (which are present in other worldwide occurrences).

Some microprobe allanite-(Ce) analyses made on the many other Ditrau samples gave Pr_2O_3, SrO_2 (up to 1%wt), Sm_2O_3, BaO and ThO_2 in small contents which were not determined in samples from Table no 3. In addition, the allanite-(Ce) has (OH) content, which also was not determined. This could be an explanation for the such low total contents of the samples presented in Table 3.

Table 1

Microprobe representative analyses of allanite-(Ce) from Fig 9, sample Dt 19/2, 2a:
2=red-black area, grown on bastnasite-(Ce); 2a=small prisms; sample Dt53/1, 3 pink prisms

2			**2a**		**1**		**3**	
Oxid	Mass%	Cation	Mass%	Cation	Mass%	Cation	Mass%	Cation
MgO	0.283	0.0757	0.297	0.0770	0.480	0.1262	1.871	0.5338
Al_2O_3	10.130	2.1439	12.916	2.6508	11.211	2.3294	4.939	1.1143
SiO_2	37.495	6.7328	39.196	6.8255	39.509	6.9655	35.143	6.7276
CaO	11.079	2.1316	10.291	1.9200	10.113	1.9103	8.293	1.7009
FeO	20.561	3.0877	16.056	2.3383	15.527	2.2893	25.451	4.0747
La_2O_3	9.755	3.0877	8.262	0.5306	9.389	0.6105	11.572	0.8171
Ce_2O_3	10.696	0.7032	12.982	0.8277	13.770	0.8888	12.731	0.8923
Total cations		15.5207		15.1699		15.1201		15.8606

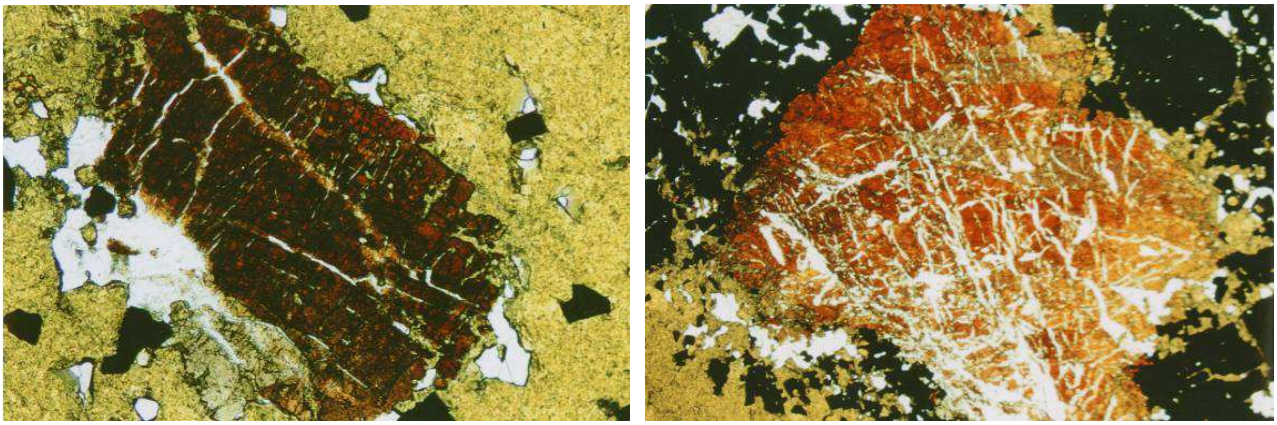

Fig. 10. Allanite-(Ce) (red) associated with sphalerite (yellow), Dt26; see it composition in Table 2 (left); allanite-(Ce) (yellow orange) associated with pyrite (black) with sphalerite veins, sample DT55, NII (right).

Table 2

Microprobe representative analyses of allanite-(Ce), sample Dt18/3-8, 11-15 (Hirtopanu *et al.*, 2010)

Oxides%	**3**	**4**	**5**	**6**	**7**	**8**	**11**	**12**	**13**	**14**	**15**
SiO_2	27.937	28.613	28.579	28.552	28.691	28.433	27.894	27.033	28.156	28.289	28.399
CaO	7.324	7.468	7.904	7.809	7.598	7.881	7.648	7.485	7.454	7.497	7.482
Al_2O_3	12.048	10.940	11.324	11.278	10.892	10.955	10.564	10.524	9.920	9.938	11.265
MgO	0.827	0.952	0.778	0.794	0.563	0.540	0.912	0.936	0.912	0.905	0.407
P_2O_5	0.151	0.139	0.143	0.149	0.152	0.165	0.164	0.140	0.113	0.139	0.179
Fe_2O_3	17.175	18.650	18.439	18.365	18.748	19.386	18.544	18.156	20.164	20.094	18.944
ThO_2	0.060	0.181	0.134	0.093	0.068	0.155	0.155	0.107	0	0	0
La_2O_3	8.310	8.445	9.431	9.568	8.318	8.863	8.460	8.372	8.488	8.356	8.363
Ce_2O_3	14.256	14.318	14.205	14.350	15.316	14.477	14.421	14.607	14.590	14.685	14.427
Pr_2O_3	1.066	1.130	0.887	0.910	0.910	1.079	1.093	1.177	0.953	1.027	1.047
PbO	0.365	0.025	0.018	0.071	0.035	0.121	0	0	0	0	0
MnO	2.417	2.346	2.303	2.344	1.909	1.973	2.106	2.166	2.024	2.125	2.466
Gd_2O_3	0.321	0.239	0.161	0.015	0.058	0.067	0.093	0.113	0.304	0.236	
Sm_2O_3	0.463	0.549	0.210	0.416	0.295	0.356	0.494	0.655	0.414	0.481	0.366
Nd_2O_3	3.927	4.106	2.792	3.008	3.206	3.336	3.820	3.840	3.707	3.625	3.453
O	61.68	61.70	61.70	61.69	61.82	61.75	61.68	61.62	61.71	61.71	61.77
Total	96.649	97.896	97.337	97.717	96.597	97.521	96.279	95.254	97.405	97.783	97.232

Table 3

Micrprobe representative allanite-(Ce) analyses Samples Dt19/ 16; 2007/10C/26, 27, 28, 35; Dt8/1, 2, 3, 4, 5, 6, 26, 27

Points	**16**	**26**	**27**	**28**	**35**	**1**	**2**	**3**	**4**	**5**	**6**	**26**	**27**
SiO_2	30.00	32.854	32.777	30.166	23.139	32.834	32.468	32.537	32.423	32.896	32.990	32.602	33.128
CaO	8.107	8.663	8.078	5.216	7.639	7.967	8.834	8.592	8.947	8.543	8.882	9.172	8.891
Na_2O	nd	nd	nd	nd	nd	0.679	0.497	0.600	0.435	0.564	0.480	0.339	0.324
Al_2O_3	7.931	19.371	20.310	16.497	13.188	19.594	18.894	19.049	18.521	19.286	19.193	19.197	20.128
MgO	0.53	0.393	0.566	0.711	0.085	nd	nd	nd	nd	nd	nd	nd	nd
P_2O_5	0.064	0.01	0.078	0.404	0.054	nd	nd	nd	nd	nd	nd	nd	nd
FeO		9.338	8.332	3.356	7.498	10.729	10.760	11.442	11.651	11.078	11.226	10.582	10.767
UO_2	0.008		0.016		0.023	nd	nd	nd	nd	nd	nd	nd	nd
ThO_2	0.089	0.193	0.132	0.267	1.393	nd	nd	nd	nd	nd	nd	nd	nd
La_2O_3	3.317	7.297	7.668	10.365	11.022	6.904	6.224	6.617	6.561	6.784	6.215	5.362	5.475
Ce_2O_3	13.244	12.859	11.674	18.73	18.619	11.596	12.521	13.134	13.077	11.849	12.635	13.182	12.156
Nd_2O_3	2.616	4.126	3.646	8.028	6.551	3.871	4.062	4.303	4.215	3.572	4.451	4.025	3.850
Pr_2O_3	nd	nd	nd	nd	nd	nd	nd	nd	nd	nd	nd	nd	nd
Gd_2O_3	0.86	1.048	1.036	1.821	1.562	1.134	1.298	1.357	1.360	1.202	1.291	1.031	1.236
Dy_2O_3	0.116	0.303	0.789	0.217	0.327	0.346	0.235	0.227	0.114	0.295	0.189	0.121	0.252
Yb_2O_3	0.014		0.058			0	0.005	0.055	0	0.032	0.012	0.071	0
Y_2O_3				0.04	0.054	0	0	0	0	0	0	0	0
MnO	2.288	1.601	2.288	0.726	1.022	0.855	0.924	1.174	0.925	1.370	0.829	1.028	0.598
F	0.289	0.190	0.164	0.451	3.753	0.146	0.186	0.196	0.254	0.216	0.210	0.198	0.154
Total	98.567	98.140	97.349	95.979	95.928	95.847	96.149	98.147	97.825	96.834	97.843	96.051	96.080

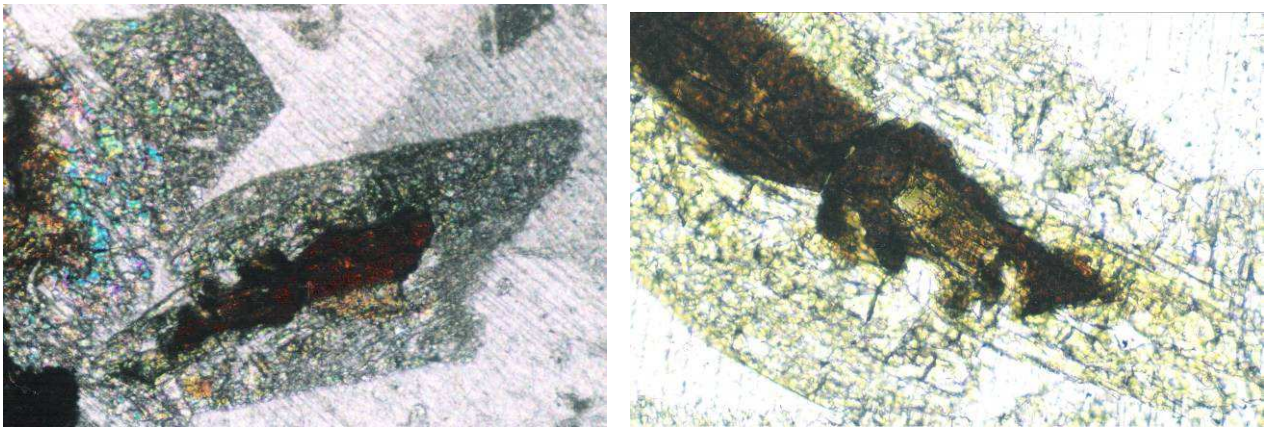

Fig. 11. Allanite-(Ce) (red) grown on monazite-(Ce) (grey green) or monazite-(Ce) grown on allanite-(Ce) (?) in calcite (grey white/grey yellow), N+ (left) and NII (right), sample Dt44.

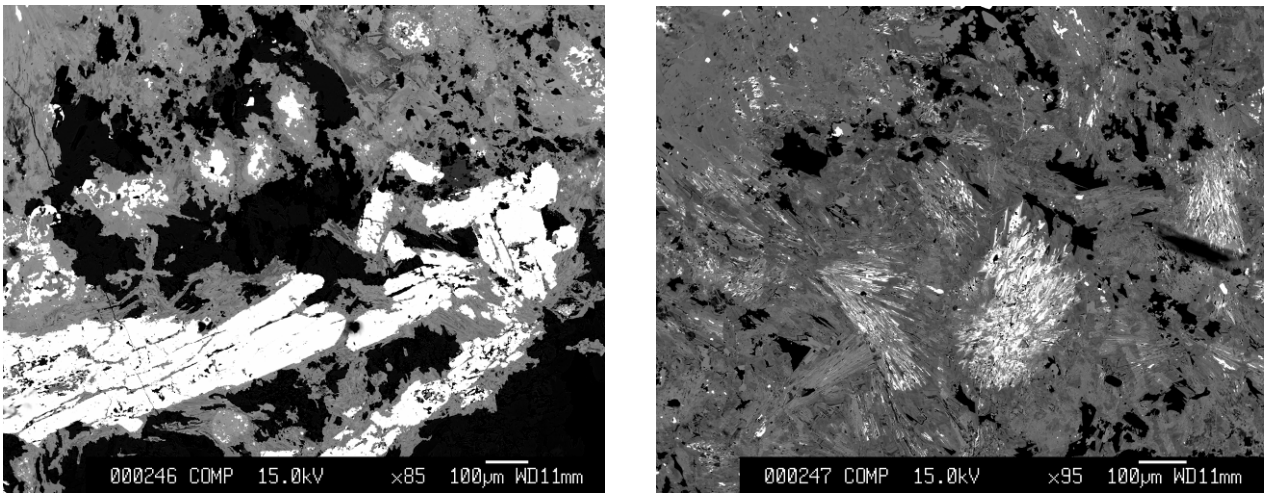

Fig. 12.BSE image of monazite-(Ce) (white prisms) substituted by allanite-(Ce) (grey, with oscillatory composition) calcite (black) (left); cerite-(Ce) (white relics) substituted by allanite-(Ce) (grey), calcite (black), sample Dt2.

The presence and concentration of REE in hydrothermal fluids are mainly controlled by temperature, pressure and composition of the fluid phase, combined with crystallochemical factors. The hydrothermal monazite-(Ce) (Figure 11) has been transformed into allanite-(Ce), although the situation could also be the reverse. This alteration was ascribed to interaction of monazite/allanite with late silicate-bearing solutions. The allanite-(Ce) /monazite-(Ce) alteration may be enhanced by damage of the crystal structure caused by the radioactive decay of alpha-emitting actinides (U,Th). In the Figure 11 the monazite-(Ce) seems to be grown on allanite-(Ce), probable because the sudden increase in the PO_4^{3-} concentration in the fluid. The allanite-(Ce) supported an interaction with late phosphate-bearing solutions. In the Figure 12 (left), the reverse process has been happened: the monazite-(Ce) is substituted by allanite-(Ce) with variable REE contents, reflected in different grey shades: light grey, more REE, dark grey, low REE. In this last case the Si activity in the fluid was very high, to permit the allanite formation on monazite. Transformations could take place among minerals belonging to the same group, *e.g.* REE-silicates. In Figure 14, the tornebohmite-(Ce) is substituted by allanite-(Ce). The mineralizing solutions suffered probable a REE-diminution content, the allanite-(Ce) having lower REE contents than törnebohmite-(Ce) (Table 4). Also, in the Figure 12 (right) the cerite-(Ce) is substitiuted almost totally by allanite-(Ce) with low REE content.

Törnebohmite (Ce), $(Ce,La)_2Al(SiO_4)_2(OH)$, monoclinic, pseudohexagonal. In thin sections there occurs as fine grained, massive, of few mm in size, and very strong pleochroism, from light rose to greenish yellow, bluish green, green (Figure 13). It has a refringence around 1.85, higher than cerite, and has no cleavage.

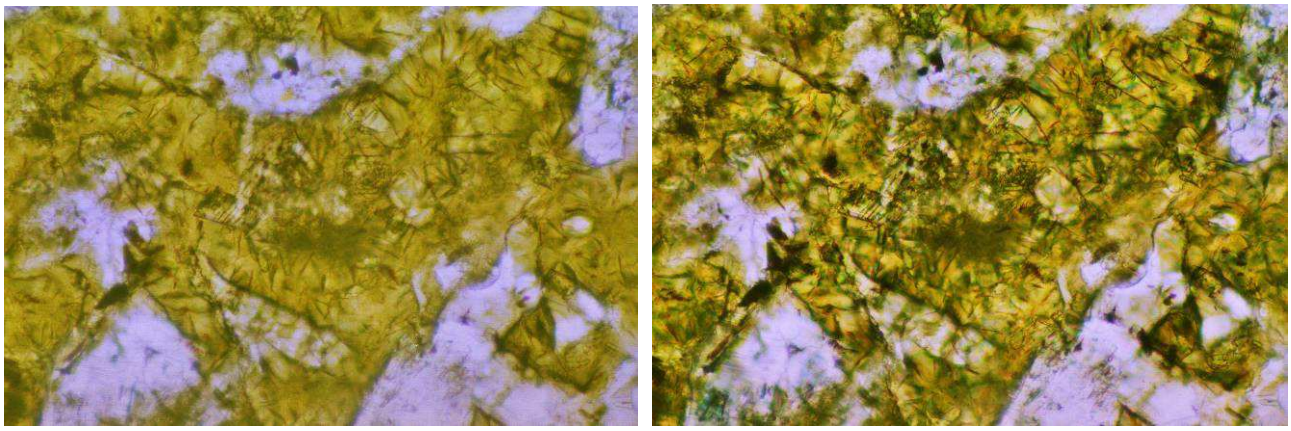

Fig. 13. Törnebohmite-(Ce) (yellow-olive) with small cerite-(Ce) (black) relics, NII (left) and N+ (right), sample Dt 37. See its chemical composition in Table 4.

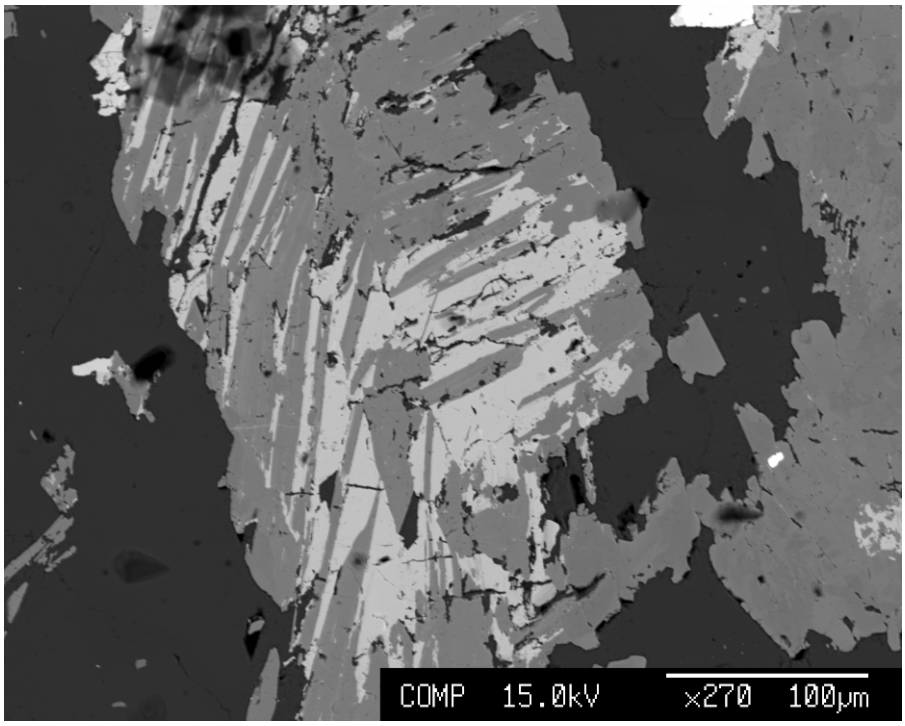

Fig. 14. Allanite-(Ce) (grey) with törnebohmite-(Ce) relics (white), calcite (black), sample DT37/3. See their chemical compositions in Table 4.

Table 4

Representative microprobe analyses of törnebohmite-(Ce) and allanite-(Ce), samples törnebohmite-(Ce) Dt37/3, 4, 5 and allanite-(Ce) Dt37/6 from Figure 11

	3		**4**		**5**		**6**	
Element	**Mass%**	**Cation**	**Mass%**	**Cation**	**Mass%**	**Cation**	**Mass%**	**Cation**
MgO	1.789	0.6119	1.537	0.5007	1.204	0.4038	2.114	0.5821
Al_2O_3	5.968	1.6145	7.548	1.9500	6.344	1.6819	6.793	1.4792=
SiO_2	27.378	6.2843	30.007	6.5778	29.062	6.5375	36.441	6.7332
CaO	0.600	0.1475	0.347	0.0815	0.174	0.0419	8.892	1.7604
FeO	1.837	0.3527	0.314	0.0576	1.848	0.3476	24.919	3.8502
La_2O_3	30.024	2.5418	30.053	2.4297	30.228	2.5080	9.131	0.6223
Ce_2O_3	32.405	2.7232	30.199	2.4236	31.140	2.5646	11.710	0.7921
Total cations		14.2759		14.0206		14.0852		15.8200

Törnebohmite-(Ce) could be a result of variation of concentrations of both Si and REE activities in the fluid, and the lowering of its temperature. The activity of the Si increases and that of the RRE decreases. The törnebohmite-(Ce), has high La_2O_3 and Ce_2O_3 contents in respect to secondary allanite-(Ce) (Table 4). Its chemical composition differs from cerite-(Ce), $(Ce,La,Ca)_9(Mg,Fe^{2+})Si_7(O.OH,F)_{28}$, in having some Al and very high La content. The törnebohmite-(Ce) forms in the environment without fluorine and probably, under relatively reducing conditions. The chevkinite-(Ce), $(Ce,La)_4(Ti,Fe)_5O_8(Si_2O_7)$, occurs under relatively oxidized conditions and at high Ti activity in the fluid. When the mineralizing fluid has also some PO_4^{3-}, beside Si, britholite-(Ce), $(Ce,Ca)_5(SiO_4,PO_4)_3(OH,F)$ can form in these associations. Because the natural hydrothermal solutions have very complex chemical composition, the formation of these minerals are most likely to be more complicated, than we have stated above.

Chevkinite-(Ce), (Ce, Nd, La, Ca) $(Fe^{2+}, Mg)_2(Ti,Fe^{3+})_3 Si_4O_{22}$, monoclinic. It occurs accessorily as small elongated lamellar, lenticular or stubby prismatic crystals, also in massive compact grains. In transmitted light it has a dark reddish brown to black colour and a strong pleochroism from deep redish brown to dark brown and opaque. The refringence and birefringence are higher than those of allanite-(Ce). It has a medium 2V, being optically negative and shows no cleavage. The chemical composition of chevkinite-(Ce), determined with microprobe is: SiO_2 = 18.77, Al_2O_3 = 1.396, TiO_2 = 15.893, FeO = 13.184, Ce_2O_3 = 36.084, CaO=0.510, Nd_2O_3 =6.408, Pr_2O_3=7.755(wt%). The SiO_2, TiO_2 and Ce_2O_3 are the main oxides in its composition. It has no La_2O_3, but Nd_2O_3 and Pr_2O_3 are present at lower contents than Ce_2O_3. The FeO is always present. Having TiO_2 content, chevckinite-(Ce) occurs frequently associated with niobian rutile, ilmenite, ilmenorutile, ferrocolumbite; also it could be associated with bastnäsite-(Ce), aeschynite-(Ce), aeschynite-(Nd), monazite-(Ce), allanite-(Ce) and calcite/quartz, in Jolotca area.

Cerite-(Ce) (Ce, La, Ca)$_9$ (Mg, Fe^{2+}) Si_7 (O, OH, F)$_{28}$, hexagonal. It forms pseudooctahedral or hexagonal crystals of a few mm in size, also massive. In thin sections it has a pleochroism from pale lavender brown, grey, red to colorless, without cleavage. Optically it is uniaxial (+). It has a refringence around 1.8, being higher than that al allanite-(Ce). It is associated with bastnäsite-(Ce), allanite-(Ce), monazite-(Ce). In respect to the allanite, the cerite was formed earlier. The textural relations between these minerals, shows the substitution of cerite by allanite. It is closely associated with bastnasite, in alternate microscopic bands, the two minerals being apparently contemporaneous. In some areas the cerite and bastnäsite are intimately intergrown with indistinguishable relationships, however, the cerite seems to be older than bastnäsite.

Being a hydrated mineral, the cerite-(Ce) contains theoretically until 3%wt (OH), which was not determined. In the other occurrences in the world, the cerite-(Ce) has small MnO, BaO, Na_2O, K_2O, TiO_2 and SO_3 contents, which also were not determined here.

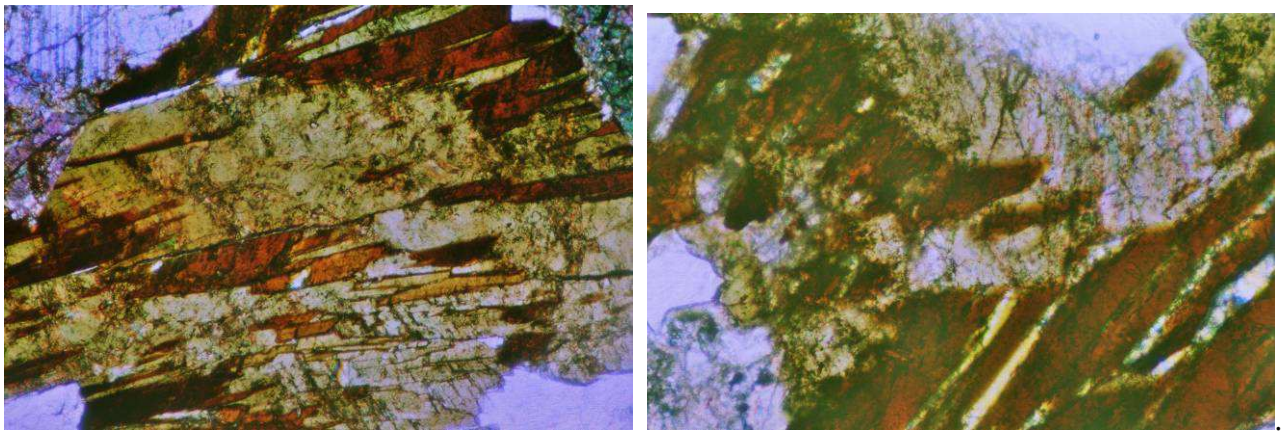

Fig. 15.Chevkinite-(Ce) (red, lens) substituted by törnebohmite-(Ce) (yellow pink green), NII, Dt212; Chevkinite-(Ce), (red) relics in törnebohmite-(Ce) (pink green), NII, Dt57; See its chemical analyses in Table 4.

Table 5
The microprobe analyses of cerite-(Ce); sample Dt212/52, 58-60, 63, 66

Oxides%	**52**	**58**	**59**	**60**	**63**	**66**
SiO_2	23.571	23.466	23.673	23.530	23.686	23.122
CaO	1.84	1.553	1.933	2.057	0.238	1.679
Al_2O_3	0	0.012	0.007	0.260	0	0.013
MgO	1.933	1.996	1.847	2.046	1.729	1.832
P_2O_5	0.017	0.013	0.038	0.053	0	0.033
FeO	0.429	0.457	0.390	0.334	0.540	0.427
UO_2	0.017	0.002	0	0	0.018	0.002
ThO_2	0	0.018	0.022	0.024	0.961	0.127
La_2O_3	18.33	16.408	17.934	18.000	15.862	16.524
Ce_2O_3	31.778	30.842	31.768	31.541	30.694	30.931
Nd_2O_3	10.996	12.982	11.351	11.782	12.000	12.716
Gd_2O_3	2.347	2.453	2.456	2.398	2.447	2.534
Dy_2O_3	0.010	0	0.004	0	0	0
Yb_2O_3	0.048	0.018	0.068	0	0	0
Y_2O_3	0	0	0	0	0	0
F	2.533	2.394	2.556	2.478	2.450	2.447
B_2O_3	0.005	0	0	0	0.084	0
Total	93.844	91.941	92.524	93.073	92.441	91.357

Stillwellite-(Ce), (Ce,La,Ca)BSiO$_5$, hexagonal. It occurs very rare as rhombohedral crystals to a few mm in size. Under microscope has almost colorless to pale pink, one imperfect cleavage and a higher refringence than allanite. In Figure 13 it is displayed the EDS spectrum of stillwellite-(Ce) from sample Dt37/5. In the same point and on the same grain, there was made its microprobe analyses. It gave followings oxides (%wt): SiO_2 =8.115, CaO=0.744, La_2O_3=36.130, Ce_2O_3=44.716, Nd_2O_3=10.056, FeO=0.239. Because the boron (B_2O_3) was not determined it appears to have too high REE-contents in its chemical composition. In sample Dt212, stillwellite-(Ce) is associated with allanite-(Ce), bastnäsite-(Ce) and has some Fe content and also high REE content (Fig. 13).

Tritomite-(Ce) (?), (CeLaYTh)$_5$(Si,B)$_3$ (O,OH,F)$_{13}$, hexagonal. Under microscope it presents short prismatic grains with orange, pink or brown color, without cleavage (Fig. 14). Its refringence is around n = 1.7 Because it has no Th in its composition (Fig. 15), it is no amorphous, no isotropic and it has a good crystalline structure. In crossed nicoles, (N+) it presents a medium birefringence (Fig. 14). Tritomite-(Ce) occurs rarely being associated with sphalerite (Fig. 14) and allanite-(Ce).

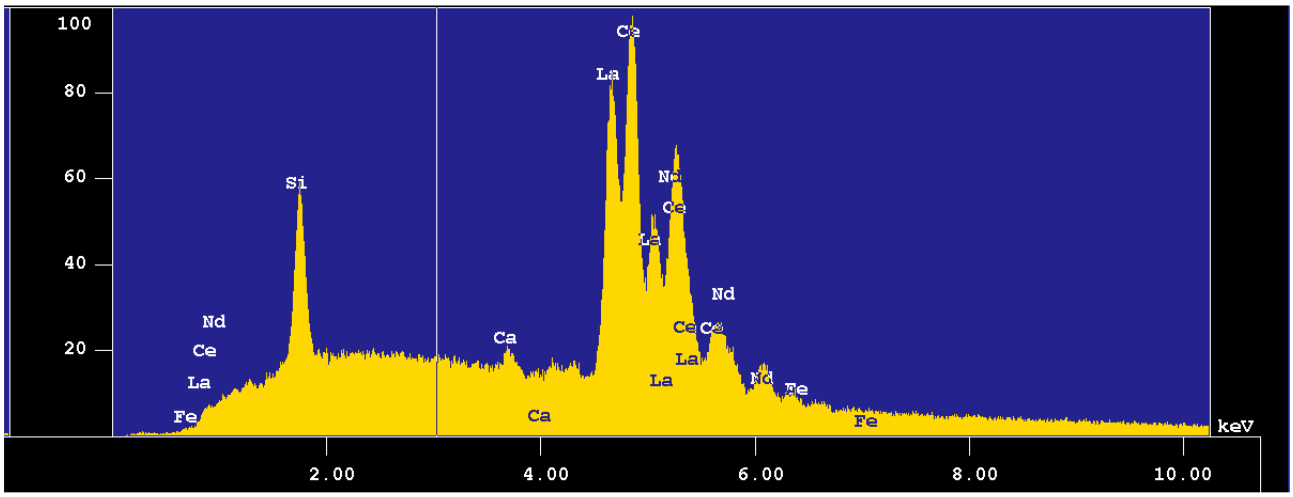

Fig. 13. EDS spectrum of stillwellite-(Ce); see up its chemical composition, sample Dt37/5.

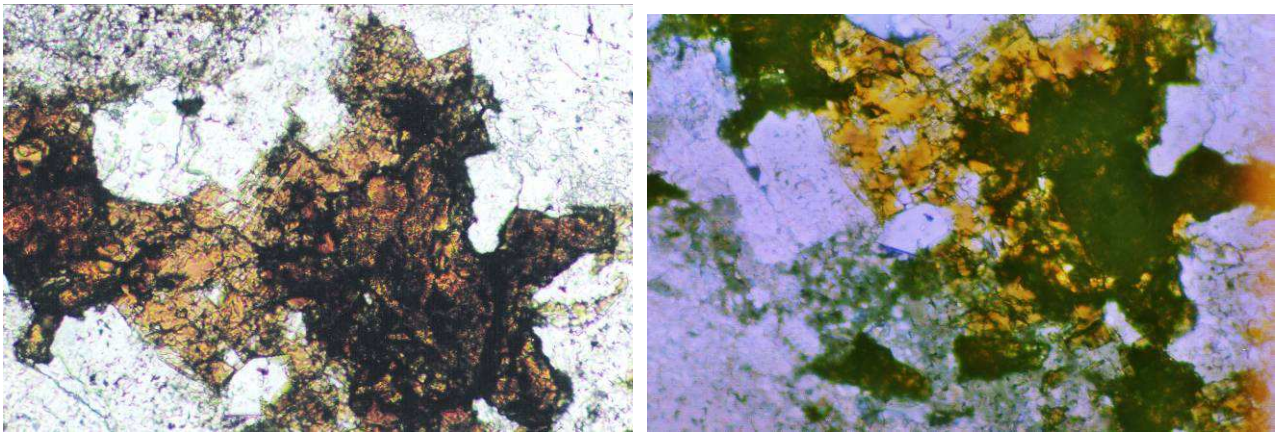

Fig. 14. Tritomite-(Ce) (?) (pink), sphalerite (red), NII (left) and N+ (right), calcite (white/grey), Dt53/4; see its EDS spectrum in Figure 15.

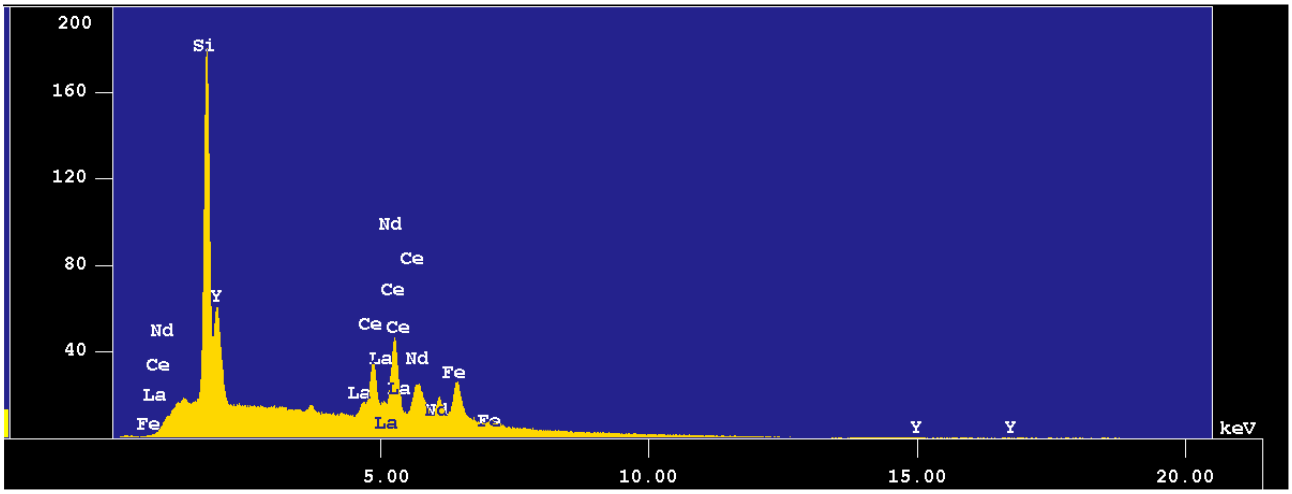

Fig. 15. EDS spectrum image of tritomite-(Ce) (?), Dt 53/4.

The textural relations of the RRE-silicates in the Ditrau suggest that cerite-(Ce) is the primary lanthanide mineral, which formed earlier than bastnasite-(Ce) and allanite-(Ce). So, allanite-(Ce) is secondary in relation to cerite-(Ce). The last one, generally, forms from silica undersaturated fluids, occurring in assemblages without quartz, such as in the Jolotca area. Also, cerite-(Ce) contains fluorine in its chemical composition, and some CaO and MgO are present in small quantities (Table 5). Some fluorine (F) had been inherited in allanite-(Ce) by its neoformation on cerite-(Ce). Like in the case of thörnebohmite-(Ce) substitution by allanite-(Ce), the transformation of the cerite-(Ce) in allanite-(Ce) was happened because some fluctuations in the avaibility of SiO_2 and in REE-bearing fluids. Allanite-(Ce) is formed at conditions with higher SiO_2 activity and higher concentrations of Al, Ca and Fe than conditions favorable for the crystallization of cerite-(Ce).

CONCLUSIONS

The rare elements minerals determined in DAIC, belong to the following 4 mineral classes: REE- Carbonates, Nb,Ta, REE–Oxides, REE-Phosphates and REE-Silicates. The allanite-(Ce) belongs to silicates class among other, like chevkinite-(Ce), törnebohmite-(Ce), cerite-(Ce), britholite-(Ce), stillwellite-(Ce) (?), tritomite-(Ce), thorite, thorogummite and zircon. It occurs as mineral constituient of the ore, showing big prismatic crystals and many generations. The chemical composition shows high Fe_2O_3 content and a diminution of REE content from old to new allanite-(Ce) generations. The high Fe_2O_3 content indicates an oxidizing conditions of allanite-(Ce) formation.

The allanite-(Ce) is associated closely with REE-carbonates, REE-phoshates and with other REE-silicates present in the DAIC. Also, the

intergrowth of allanite-(Ce) with sulphides, specially with sphalerite and pyrite, is very common, being linked by metallogenetically process. The textural relations between diverse REE-minerals, showed that the-allanite-(Ce) has many generations, being substituted/neoformed by/on many REE minerals. Replacement of earlier REE minerals by later REE minerals is common in DAIC such as the replacement of monazite by bastnasite+apatite and reaction of bastnasite and apatite to form monazite and fluorite. Also, the neoformation of allanite-(Ce) on monazite and bastnasite-(Ce) occurs frequently.

The substitutions of REE minerals belonging to the same class took place in DAIC. The bastnasite-parisite transformation is very likely to result from variations of either Ca^{2+} and CO_2^{2-} activities in the fluids. The substitutions among the REE-silicates were described: allanite-(Ce) substitutes törnebohmite-(Ce), chevkinite-(Ce) and cerite-(Ce), by diminution of REE-content, because some fluctuations in the availability of SiO_2 and in REE-bearing fluids. Allanite-(Ce) is formed under conditions with higher SiO_2 activity and higher concentrations of Al, Ca and Fe than that the conditions favourable for the crystallization of the other REE-silicates shown above. Some changes in pH, oxidizing conditions and T have probable occurred, and in the REE concentrations, as well.

The DAIC display extensive evidence of hydrothermal alteration, (natrolitisation, albitisation etc.), which is widespread in those parts of the massive that is most enriched in HFSE-, high field-strength elements (Zr, Nb, U, Y, REE) and in halogens, especially fluorine. The REE are transported mainly as fluoride complexes in hydrothermal fluids derived from alkaline/ peralkaline magmas. This is supported by the fact that the principal REE ore mineral is bastnasite-(Ce), and the fluorite is an important gangue mineral in DAIC. The sulphate and carbonate ligands may play an important role in REE transport and their deposition, as carbonate and sulphate REE complexations. For many years, the REE had been considered to be immobile in hydrothermal fluids. However, now is has become increasingly apparent that the REE can be concentrated to ore grades via hydrothermal processes. It is known, that the alkaline igneous rocks arguably contain the highest concentrations of HFSE of any igneous rock type, and intrusions of such rocks commonly host exploitable resources of these elements.Now, the DAIC hosts Ti, Nb, Ta, Th, U, Y, Zr, and REE mineralization, being a site of a subeconomic deposit.

ACKNOWLEDGEMENTS

Many thanks to the Roumanian Academy for material support, i.e. the grants No 133/2007-2008 and No 134/2007-2008, allowing us to work in the modern laboratories of Exeter University, Camborne School of Mines, Cornwall, UK. We thank to Prof. G. Udubasa, at Bucharest University, for helpful suggestions on ways to improve the text. Also, we are very grateful to Prof. Peter Gromet, at Brown University, Providence, RI, USA, for high resolution scanning of the Dt6 and Dt18 polished thin sections with allanite-(Ce), and for the photos shown in Figures 4, 6, 7, 8, 9, 10, 11.

REFRERENCES

1. Anastasiu N., Constantinescu E. Observatii mineralogice in rocile sienitice din masivul Ditrau, Comunicari Geologice, Tipografia Universitatii Bucureşti (1976).
2. Barnes H.L., Solubility of ore minerals, in Geochemistry of of hydrothermal ore deposits (ed. H.L. Barnes, Wiley & Sons, New York, 1979, pp. 404-60.
3. Constantinescu, E. Mineralogy in the system of the Earth, London: Imperial College Press. 1999, 384p.
4. Gieré, R., Formation of rare earth minerals in hydrothermal systems, in Rare Earth Minerals, Chemistry, origin and deposits, Edited by Adrian P.Jones, Frances Wall and Terry Williams, 1996, pp. 106-150.
5. Hîrtopanu P., Bermanec V., Udubaşa G., Melgarejo J.C., Monazite and allanite from the Ditrau alkaline massif East Carpathians, Romania,The 4th Baia Mare Symposium of the GSR, Ann.Inst.Geol., v.72, Special Issue, Bucureşti, 2000, p. 41.
6. Hirtopanu Paulina, Udubasa G., Hartopanu I., Some old and new minerals from Ditrau alkaline massif and their genetical implications, Anniversary Symposium, Univ. of Bucharest, 2003, p. 29.
7. Hirtopanu Paulina & Udubasa G., Mineralogy of a “sacred monster”, the Ditrau alkaline massif, East Carpathians, Romania, 6th Symposium on mineralogy, Studia Univ. Babes-Bolyai Cluj-Napoca, Geologia, Special Issue, 2003, p. 47.
8. Hirtopanu, P. & Udubaşa, G. REE-bearing minerals at Ditrău, Rom. J. Mineral., **82**, 2004, 184–187.
9. Hirtopanu Paulina**,** One hundred minerals for one hundred years (dedicated to the Centennial of the Geological institute of Romania), 3rd Conference on Mineral Sciences in the Carpathians, Miskolc Hungary, Acta Min. Petr. Univ. Szeged Hungary, Abstr.Series 5, 2006a, p 86.
10. Hirtopanu Paulina, One hundred minerals for one hundred years (dedicated to the Centennial of the Geological institute of Romania), 3rd Conference on Mineral Sciences in the Carpathians, Miskolc Hungary, Acta Min.Petr.Univ.Szeged Hungary, Abstr.Series 5, 2006b, p 86.
11. Hirtopanu Paulina, Jens C. Andersen & Robert J. Fairhurst: Nb, Ta, REE(Y), Ti, Zr, Th, U and Te rare element minerals within the Ditrau alkaline intrusive complex, Eastern Carpathians, Romania, Mineralogy of Szekelyland, Eastern Transylvania, Romania", 2010a,

Edited by Sandor Szakall and Ferenc Kristaly, Tg Mures, 2010a, pp. 89-128.

12. Hirtopanu Paulina, Andersen C. Jens & Fairhurst J. Robert, Nb, Ta, REE(Y), Ti, Zr, Th, U and Te rare element minerals within the Ditrău alkaline intrusive complex, East Carpathians, Romania, 20th General Meeting oh the International Mineralogical Association (IMA), 21-27 August 2010, Budapesta, Hungary, CD Abstracts, 2010b, pp.570.
13. Jakab, Gy., Geologia masivului alcalin de la Ditrău. Miercurea Ciuc: Ed. Pallas-Akademia. 1998, 297p.
14. Krautner H., Bindea G., The Ditrau alkaline intrusive complex and its geological environment. Rom. J. Min, 77, supp 3, (1995), pp 44, Bucuresti.
15. Miyawaki, R., and Nakai, I., Crystal structures of rare-earth minerals. Rare Earths, No21, 1993, p. 1-18.
16. Streckeisen, A., On the structure and origin of the Nephelinsyenite Complex of Ditro (Transylvania, Roumania), Rep. 21th IGC, V. 13, 1960, pp. 228-238.